REPORT 1024

CALCULATION OF THE LATERAL CONTROL OF SWEPT AND UNSWEPT FLEXIBLE WINGS OF ARBITRARY STIFFNESS[1]

By Franklin W. Diederich

SUMMARY

A method similar to that of NACA Rep. 1000 is presented for calculating the effectiveness and the reversal speed of lateral-control devices on swept and unswept wings of arbitrary stiffness. Provision is made for using either stiffness curves and root-rotation constants or structural influence coefficients in the analysis. Computing forms and an illustrative example are included to facilitate calculations by means of the method.

The effectiveness of conventional aileron configurations and the margin against aileron reversal are shown to be relatively low for swept wings at all speeds and for all wing plan forms at supersonic speeds.

INTRODUCTION

Adequate lateral control constitutes one of the more significant design requirements for airplanes. The ability of the airplane to enter a roll is determined by the control power and is measured by the maximum available rolling moment resulting from lateral-control deflection. A measure of the degree of lateral maneuverability is the helix angle at the wing tips corresponding to the highest rate of roll; the lateral maneuverability depends both on the control power and the damping in roll.

The control power and the damping in roll are affected by structural flexibility. Control deflection ordinarily gives rise to aerodynamic loads which tend to deform the wing structure in such a way as to reduce the loads on it and thus to reduce the control power. If the dynamic pressure of the air stream is sufficiently high, the amount of lift which results from the structural deformation may be sufficient to nullify the effect of the control deflection. The speed and dynamic pressure corresponding to this condition are known as the aileron reversal speed or reversal dynamic pressure, since at a slightly higher dynamic pressure a control deflection in a given direction would result in a rolling moment in a direction opposite to that of the moment on a similar rigid wing.

The present report is concerned with an analysis of these problems for swept and unswept wings of arbitrary stiffness. The method is based on the analysis of loading of flexible wings presented in reference 1. Since suitable aerodynamic influence coefficients are not yet available for antisymmetric lift distributions, aerodynamic-induction effects on the lift distribution are taken into account only as an over-all correction and as a slight reduction of the load at the tip, as in reference 1. The method is formulated in such a manner, however, that aerodynamic influence coefficients may easily be included as soon as they become available.

The numerical analysis required in any given practical case constitutes an extension of the calculations outlined in reference 1. The computing forms for the additional calculations required for an analysis of lateral-control effectiveness or reversal are included in the present report. Their use is described in the section entitled "Application of the Method," which may be read without reference to the derivation of the method. The material presented in reference 1 which is pertinent to the present analysis is included herein. As an example illustrating the method, the lateral-control effectiveness and reversal of the wing considered in reference 1 are analyzed in this report. The reversal speeds of several wings derived from this wing by shifting the elastic axis and rotating the wing are calculated to demonstrate some general effects of sweep on the aileron reversal speed.

SYMBOLS

A	aspect ratio (b^2/S)
$[A]$, $[A^\dagger]$	aeroelastic matrices defined by equations (7) and (10)
$[\overline{A}]$, $[\overline{A}^\dagger]$	auxiliary aeroelastic matrices defined by equations (8) and (11)
$[A_R]$	aileron-reversal matrix defined by equation (18)
a	section aerodynamic center, measured from leading edge, fraction of chord
b	wing span, inches
b'	wing span less fuselage width, inches
c	chord measured parallel to the air stream, inches
c	average wing chord, inches (S/b)
c_l	section lift coefficient (l/qc)
c_{l_α}	section lift-curve slope, per radian
$c_{m_{c/4}}$	section pitching-moment coefficient referred to quarter-chord point
C_{L_α}	wing lift-curve slope, per radian

[1] Supersedes NACA RM L8H24a, "Calculation of the Effects of Structural Flexibility on Lateral Control of Wings of Arbitrary Plan Form and Stiffness" by Franklin W. Diederich, 1948.

$C_{L_{\alpha_e}}$ effective lift-curve slope for twist distributions, per radian

C_l rolling-moment coefficient $\left(\frac{\text{Rolling moment}}{qSb}\right)$

$[C_3']$ matrix converting torques due to distributed loads to torques due to concentrated torques

$[C_4']$ matrix converting bending moments due to distributed loads to bending moments due to concentrated loads

cp_δ section center of pressure due to aileron deflection measured from leading edge of chord, fraction of chord

EI bending stiffness in planes perpendicular to the elastic axis, pound-inches ^{2}

e location of elastic axis measured from leading edge, fraction of chord

e_1 dimensionless distance along chord from reference axis to section aerodynamic center $(e-a)$

e_2 dimensionless distance along chord from reference axis to section center of pressure due to aileron deflection $(cp_\delta-e)$

g factor proportional to the rolling-moment coefficient due to aileron deflection defined by equation (16)

GJ torsional stiffness in planes perpendicular to the elastic axis, pound-inches ^{2}

$[I]$, $[I']$ integrating matrices for single integration from tip to root

$[II]$, $[II']$ integrating matrices for double integration from tip to root

$[I'_1]$, $[II'_1]$ first rows of matrices $[I']$ and $[II']$, respectively

$[II'_0]$ integrating matrix defined by equation (14)

k dimensionless parameter

$$\left(\frac{(GJ)_r}{(EI)_r}\frac{b'/2}{e_{1_r}c_r\cos^2\Lambda}\tan\Lambda\right)$$

κ wing lift-curve-slope ratio $\left(C_{L_{\alpha_e}}/C_{L_\alpha}\right)$

l running air load per unit length perpendicular to the plane of symmetry, pounds per inch

M_0 free-stream Mach number

$\frac{pb}{2V}$ wing-tip helix angle

Q_{α_M}, Q_{α_T} root-twist constants

q dynamic pressure, pounds per square inch

q^* dimensionless dynamic pressure

$$\left(\frac{C_{L_\alpha}q(b'/2)^2e_{1_r}c_r^2\cos\Lambda}{(GJ)_r}\right)$$

$q^\dagger$ reduced dynamic pressure $\left(C_{L_\alpha}q\frac{b'}{2}c_r\right)$

$\bar{q}$ dimensionless dynamic pressure

$$\left(\frac{C_{L_\alpha}q(b'/2)^3c_r\tan\Lambda}{(EI)_r\cos\Lambda}\right)$$

S total wing area including part of wing covered by fuselage, square inches

s_m trace of matrix $[A_R]^m$

t running torque due to air load about axes perpendicular to the plane of symmetry, inch-pounds per inch

w fuselage width, inches

w_e distance between the effective root and the innermost complete section of the torsion box perpendicular to the elastic axis, inches

y lateral ordinate measured from plane of symmetry, inches

α_s angle of attack due to structural deformation, radians

α_δ angle of attack equivalent to unit aileron deflection $\left(\frac{dc_l/d\delta}{dc_l/d\alpha}\right)$

δ aileron deflection measured in planes parallel to the direction of flight, radians

ϵ moment-arm ratio (e_2/e_1)

η lateral distance from wing root, inches

Λ angle of sweepback (measured to the reference axis unless specified otherwise), degrees

$[\Phi_P]$ influence-coefficient matrix for wing twist in planes parallel to the air stream due to concentrated unit loads applied at the reference axis, radians per pound

$[\Phi_T]$ influence-coefficient matrix for wing twist in planes parallel to the air stream due to concentrated unit torques applied in planes parallel to the air stream, radians per inch-pound

Subscripts:

$c/2$ midchord

D divergence

fw flexible wing

i inboard end of aileron

o outboard end of aileron

p damping in roll

R reversal

R_0 reversal of unswept wing

r at root or effective root

rw rigid wing

sub subsonic

spr supersonic

w wing exclusive of fuselage

δ due to (unit) aileron deflection

Matrix notation:

$\{\ \}$ column matrix

$|\ \ |$ row matrix

$[\ \ ]$ square matrix

$\lfloor\ \ \rfloor$ diagonal matrix

$[\ ]''$ double transpose of a matrix: first about the principal diagonal, then about the other diagonal

$[1]$ unit matrix

$$[1_1'] = \begin{bmatrix} 0 & 0 & 0 & 0 & . & . \\ 1 & 0 & 0 & 0 & . & . \\ 1 & 0 & 0 & 0 & . & . \\ 1 & 0 & 0 & 0 & . & . \\ 1 & 0 & 0 & 0 & . & . \\ . & . & . & . & . & . \\ . & . & . & . & . & . \end{bmatrix}$$

DERIVATION OF THE METHOD

ASSUMPTIONS

The assumptions made in reference 1 are that all deformations and angles of attack are small and that the wing deformations either are known in the form of structural influence coefficients or can be calculated from simple beam theory in conjunction with rotations of a flexible root. In addition the assumption is made in the present report that the angle between the aileron and the wing is constant along the span of the aileron and that, in the absence of suitable aerodynamic influence coefficients, aeroelastic effects due to aileron deflection can be calculated on the basis of a modified strip theory.

AIR LOADS

The lift on a wing section of unit width parallel to the direction of flight may be expressed in terms of the loading coefficient cc_l/c_r as

$$\{l\} = qc_r\left\{\frac{cc_l}{c_r}\right\} \tag{1}$$

In the case of a wing at zero angle of attack with ailerons deflected the lift may be considered to consist of two parts: one due to structural deformation and one due to aileron deflection. The loading coefficients for these two parts are best treated separately.

The part of the lift due to the antisymmetric structural twist can be written in terms of the local values of twist as

$$\left\{\frac{cc_l}{c_r}\right\} = C_{L_\alpha}[Q_a]\{\alpha_s\} \tag{2}$$

in terms of suitable antisymmetric aerodynamic influence coefficients $[Q_a]$. Since no such coefficients are available at present, modified strip theory may be used, as in reference 1, with some saving in labor but at some sacrifice in accuracy. With this modified strip theory

$$\left\{\frac{cc_l}{c_r}\right\} = C_{L_{\alpha_e}}\left\lfloor\frac{c}{c_r}\right\rceil\{\alpha_s\} \tag{3}$$

where for subsonic speeds the approximate value of effective lift-curve slope $C_{L_{\alpha_e}}$ may be obtained from the equation

$$C_{L_{\alpha_e}} = c_{l_\alpha}\frac{A\cos\Lambda}{A+4\cos\Lambda}$$

and for supersonic speeds,

$$C_{L_{\alpha_e}} = \frac{4\cos\Lambda_{c/2}}{\sqrt{M_0^2\cos^2\Lambda_{c/2}-1}}$$

c_{l_α} being the lift-curve slope of the section perpendicular to the quarter-chord line at a Mach number equal to $M_0\cos\Lambda$.

The lift due to aileron deflection should be calculated by a fairly accurate method (see references 2 and 3). This lift distribution may be expressed as

$$\left\{\frac{cc_l}{c_r}\right\}_\delta = \alpha_\delta\delta C_{L_{\alpha_e}}\left\{\frac{cc_l}{c_rC_{L_{\alpha_e}}}\right\}_\delta$$

$$= \alpha_\delta\delta C_{L_{\alpha_e}}\left\lfloor\frac{c}{c_r}\right\rceil\left\{\frac{c_l}{C_{L_{\alpha_e}}}\right\}_\delta$$

where the coefficients $\left(\frac{c_l}{C_{L_{\alpha_e}}}\right)_\delta$ are the values of c_l calculated for a unit effective aileron deflection $\alpha_\delta\delta$ and divided by $C_{L_{\alpha_e}}$.

The combined lift due to twist and aileron deflection is then

$$\{l\} = qc_rC_{L_{\alpha_e}}\left\lfloor\frac{c}{c_r}\right\rceil\left\{\{\alpha_s\}+\alpha_\delta\delta\left\{\frac{c_l}{C_{L_{\alpha_e}}}\right\}_\delta\right\} \tag{4}$$

The torque per unit width of span is the product of the lift per unit width and the local moment arm. For the lift due to twist the moment arm is e_1c; for the lift due to aileron deflection the moment arm is $-e_2c$. (See fig. 1.) Consequently, the torque may be written as

$$\{t\} = qc_r^2C_{L_{\alpha_e}}e_{1_r}\left\lfloor\frac{e_1}{e_{1_r}}\left(\frac{c}{c_r}\right)^2\right\rceil\left\{\{\alpha_s\}-\alpha_\delta\delta\,[\epsilon]\left\{\frac{c_l}{C_{L_{\alpha_e}}}\right\}_\delta\right\} \tag{5}$$

where ϵ is the ratio of the moment arms e_2/e_1.

THE AEROELASTIC EQUATION

Method employing stiffness curves.—The lifts and torques per unit width given in the preceding section can be integrated to obtain bending moments and accumulated torques about axes perpendicular and parallel to the plane of symmetry and, hence, about axes perpendicular and parallel to the elastic axis. Integration of these torques and moments yields the twists and local dihedrals, which can be combined to yield the desired angle of attack due to

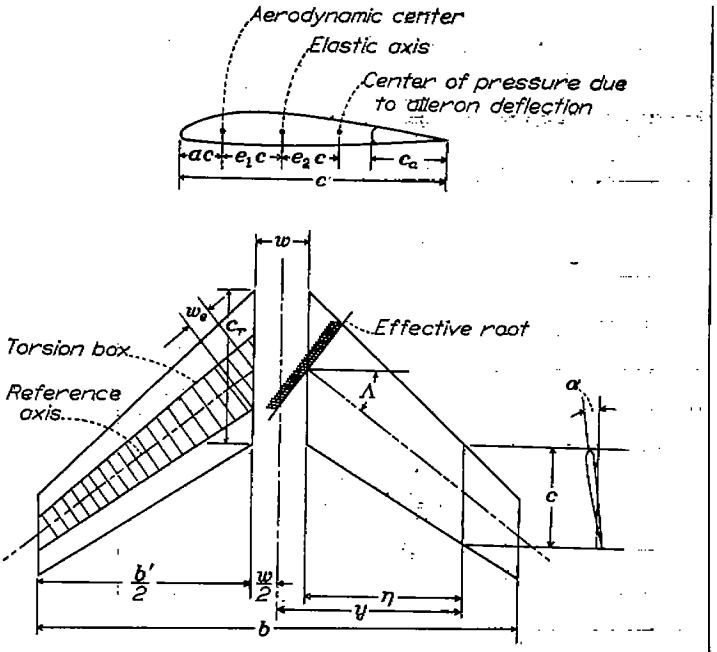

FIGURE 1.—Definition of geometrical parameters used in the analysis.

structural deformation α_s. (See reference 1.) The resulting equation is

$$\{\alpha_s\}=\kappa q^*\left\{[A]\{\alpha_s\}-\alpha_\delta\delta[\overline{A}]\left\{\frac{c_l}{C_{L_{\alpha_e}}}\right\}_\delta\right\} \tag{6}$$

where κ, the ratio of the effective to the actual wing lift-curve slope, is

$$\kappa=\frac{A+2\cos\Lambda}{A+4\cos\Lambda}$$

for subsonic flow and has a value of 1 for supersonic flow, q^* is the dimensionless dynamic pressure, $[A]$ is the aeroelastic matrix defined in reference 1 (for subsonic flow) as

$$\begin{aligned}[A]=&\left[[I]''\left[\frac{(GJ)_r}{GJ}\right]+\frac{w_e}{b'/2}(Q_{\alpha_T}-Q_{\alpha_M}\tan\Lambda)[1_1']\right.\\&\left.+\frac{(GJ)_r}{(EI)_r}\tan^2\Lambda[I]''\left[\frac{(EI)_r}{EI}\right]\right][I']\left[\frac{e_1}{e_{1_r}}\left(\frac{c}{c_r}\right)^2\right]\\&-\left[k[I]''\left[\frac{(EI)_r}{EI}\right]-\frac{w_e}{b'/2}\frac{b'/2}{e_{1_r}c_r\cos^2\Lambda}Q_{\alpha_M}[1_1']\right][II']\left[\frac{c}{c_r}\right]\end{aligned} \tag{7}$$

and $[\overline{A}]$ is an auxiliary aeroelastic matrix defined (for subsonic flow) by

$$\begin{aligned}[\overline{A}]=&\left[[I]''\left[\frac{(GJ)_r}{GJ}\right]+\frac{w_e}{b'/2}(Q_{\alpha_T}-Q_{\alpha_M}\tan\Lambda)[1_1']\right.\\&\left.+\frac{(GJ)_r}{(EI)_r}\tan^2\Lambda[I]''\left[\frac{(EI)_r}{EI}\right]\right][I']\left[\frac{e_1}{e_{1_r}}\left(\frac{c}{c_r}\right)^2\right][\epsilon]\\&+\left[k[I]''\left[\frac{(EI)_r}{EI}\right]-\frac{w_e}{b'/2}\frac{b'/2}{e_{1_r}c_r\cos^2\Lambda}Q_{\alpha_M}[1_1']\right][II']\left[\frac{c}{c_r}\right]\end{aligned} \tag{8}$$

For supersonic flow, matrices $[I]$ and $[II]$ are used instead of matrices $[I']$ and $[II']$, provided that the decrease in lift at the tip is known; otherwise, matrices $[I']$ and $[II']$ may be used in supersonic flow also as a fair approximation.

Method employing structural influence coefficients.—If the angle-of-attack changes due to unit concentrated normal loads and torques $[\Phi_P]$ and $[\Phi_T]$ have been determined in static tests of the actual structure or calculated by a method such as that of reference 4, they may be used in an aeroelastic analysis in the manner indicated in reference 1. The pertinent aeroelastic equation for the lateral-control problem is

$$\{\alpha_s\}=\kappa q^\dagger\left\{[A^\dagger]\{\alpha_s\}-\alpha_\delta\delta[\overline{A}^\dagger]\left\{\frac{c_l}{C_{L_{\alpha_e}}}\right\}_\delta\right\} \tag{9}$$

where $[A^\dagger]$ is the aeroelastic matrix defined in reference 1 as

$$[A^\dagger]=\left[e_{1_r}c_r[\Phi_T][C_3']\left[\frac{e_1}{e_{1_r}}\left(\frac{c}{c_r}\right)^2\right]+[\Phi_P][C_4']\left[\frac{c}{c_r}\right]\right] \tag{10}$$

$[\overline{A}^\dagger]$ is an auxiliary aeroelastic matrix defined by

$$[\overline{A}^\dagger]=e_{1_r}c_r[\Phi_T][C_3']\left[\frac{e_1}{e_{1_r}}\left(\frac{c}{c_r}\right)^2\right][\epsilon]-[\Phi_P][C_4']\left[\frac{c}{c_r}\right] \tag{11}$$

$q^\dagger$ is the reduced dynamic pressure defined by

$$q^\dagger=C_{L_\alpha}q\frac{b'}{2}c_r$$

and the load-conversion matrices $[C_3']$ and $[C_4']$ are defined and given in reference 1.

SOLUTION OF THE AEROELASTIC EQUATION

Calculation of the control effectiveness.—The aerodynamic loading corresponding to a given aileron deflection at a given dynamic pressure can be obtained by writing equation (6) or equation (9) in the form

$$[[1]-\kappa q^*[A]]\{\alpha_s\}=-\kappa q^*\alpha_\delta\delta[\overline{A}]\left\{\frac{c_l}{C_{L_{\alpha_e}}}\right\}_\delta \tag{12}$$

Once the right-hand side of equation (12) is evaluated it may be regarded as a set of knowns which in conjunction with the coefficients of the matrix $[[1]-\kappa q^*[A]]$ permits a solution for the unknowns $\{\alpha_s\}$. The loading corresponding to $\{\alpha_s\}$ may then be obtained from equation (4) and hence the net rolling moment due to aileron deflection and the resulting wing deformations:

$$\text{Rolling moment}=2\left(\frac{b'}{2}\right)^2[II'_0]\{l\} \tag{13}$$

where

$$[II'_0]=[II'_1]+\frac{w}{b'}[I'_1] \tag{14}$$

As indicated in reference 1, the solution of the set of simultaneous equations represented by equation (12) may be carried out by any conventional method of solving simultaneous equations or by an iteration procedure, the choice of method depending primarily on the preference of the computer.

Calculation of the aileron reversal speed.—The aileron reversal speed can be obtained by calculating the rolling moment due to aileron deflection, as indicated in the

preceding paragraph, and plotting it against the speed or dynamic pressure. The value or values of the speed or dynamic pressure for which the rolling moment is zero constitute the aileron reversal speeds or dynamic pressures. However, a more direct procedure, similar to that used to find the divergence speed in reference 1, can be derived as follows.

The term $\alpha_\delta \delta \left\{\frac{c_l}{C_{L_{\alpha_e}}}\right\}_\delta$ in equation (12) can be expressed in terms of $\{\alpha_s\}$ by means of equations (4) and (13) since at the aileron-reversal condition the rolling moment is equal to zero. Hence,

$$\lfloor II'_0 \rfloor \left\lfloor \frac{c}{c_r} \right\rceil \left\{ \{\alpha_s\} + \alpha_\delta \delta \left\{ \frac{c_l}{C_{L_{\alpha_e}}} \right\}_\delta \right\} = 0$$

or

$$\alpha_\delta \delta = -\frac{\lfloor II'_0 \rfloor \left\lfloor \frac{c}{c_r} \right\rceil \{\alpha_s\}}{\lfloor II'_0 \rfloor \left\lfloor \frac{c}{c_r} \right\rceil \left\{ \frac{c_l}{C_{L_{\alpha_e}}} \right\}_\delta}$$

Multiplying both sides of this equation by $\left\{\frac{c_l}{C_{L_{\alpha_e}}}\right\}_\delta$ yields

$$\alpha_\delta \delta \left\{ \frac{c_l}{C_{L_{\alpha_e}}} \right\}_\delta = -\frac{1}{g} \left\{ \frac{c_l}{C_{L_{\alpha_e}}} \right\}_\delta \lfloor II'_0 \rfloor \left\lfloor \frac{c}{c_r} \right\rceil \{\alpha_s\} \tag{15}$$

where

$$g = \lfloor II'_0 \rfloor \left\lfloor \frac{c}{c_r} \right\rceil \left\{ \frac{c_l}{C_{L_{\alpha_e}}} \right\}_\delta \tag{16}$$

Substitution of equation (15) in equation (12) yields

$$\{\alpha_s\} = \kappa q^* [A_R] \{\alpha_s\} \tag{17}$$

where the aileron-reversal matrix $[A_R]$ is defined by

$$[A_R] = [A] + \frac{1}{g} [\overline{A}] \left\{ \frac{c_l}{C_{L_{\alpha_e}}} \right\}_\delta \lfloor II'_0 \rfloor \left\lfloor \frac{c}{c_r} \right\rceil \tag{18}$$

The value of the dimensionless dynamic pressure κq^* at reversal can be found by iterating equation (17) or by expanding the determinant of the matrix $[[1] - \kappa q^* [A_R]]$ and setting the resulting polynomial in κq^* equal to 0, as described in reference 1.

APPLICATION OF THE METHOD

SELECTION OF THE PARAMETERS

The geometric and structural parameters used in the calculation of the lateral-control effectiveness and related aeroelastic properties of a wing are the same as those used in the calculations of the aerodynamic loading described in reference 1. If the root-rotation constants are different for symmetric and antisymmetric loadings, those for antisymmetric loadings should be used for calculating the $[A]$ matrix used in this report. Similarly, the section lift-curve slope, wing lift-curve slopes, and local aerodynamic-center values are chosen for the Mach number of interest, as described in reference 1, except for the calculation of the aileron reversal speed, as discussed in the section entitled "Calculation of the Aileron Reversal Speed."

The values of α_δ and cp_δ are best obtained from experimental section data at the appropriate Mach number $M_0 \cos \Lambda$. These values, in terms of commonly available quantities, are

$$\alpha_\delta = \frac{\frac{dc_l}{d\delta}}{\frac{dc_l}{d\alpha}}$$

and

$$cp_\delta = 0.25 - \frac{\frac{dc_{m_{c/4}}}{d\delta}}{\frac{dc_l}{d\delta}}$$

Theoretical thin-airfoil values of these parameters are given in figure 2 for subsonic and supersonic speeds. Insufficient information exists at present to permit an accurate correction of these data for finite-span effects in all cases. In a qualitative sense, the section value of α_δ is known to be a useful approximation to the actual value required in the calculations of this report, except for wings of very low aspect ratio, for which the value of α_δ tends to be somewhat larger than the section value.

The values of cp_δ on a wing tend to be further rearward than the values obtained from section data at subsonic speeds. The finite-span values may be estimated by calculating lift distributions for a given aileron deflection both by unmodified strip theory and by a rational finite-span method, such as that of reference 2 or of reference 3; if the local lift given by strip theory is assumed to act at the section value of cp_δ, and if the difference in the lifts given by the two theories is assumed to act at the local aerodynamic center, the chordwise location of the resultant of these two forces may be considered to be the three-dimensional value of cp_δ. On the basis of this approximation $e_2 = -e_1$ at all points on the wing not covered by the aileron.

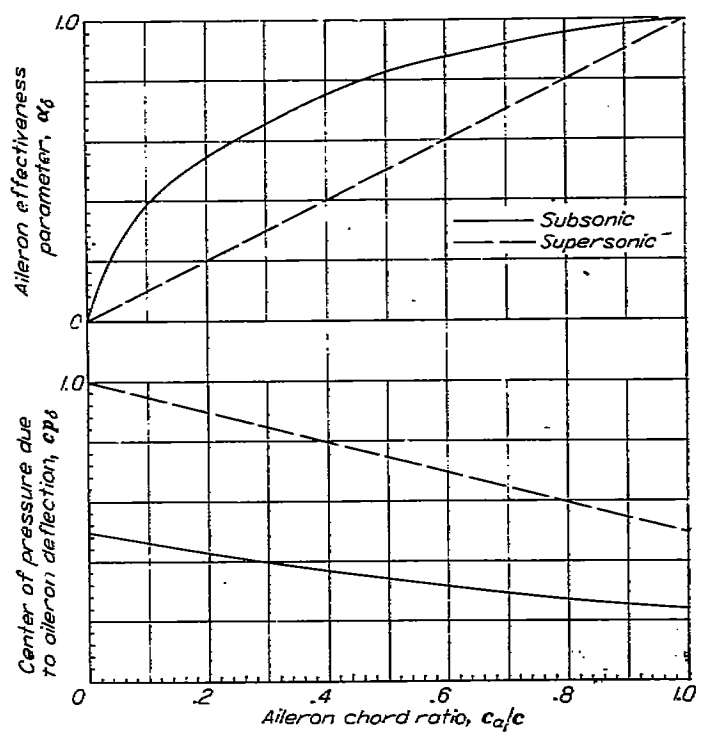

FIGURE 2.—Theoretical thin-airfoil values of the aileron force parameters.

The values of $\left\{\frac{c_l}{C_{L_{\alpha_e}}}\right\}_\delta$ required in this report may also be obtained for subsonic speeds by the methods of references 2 or 3 by calculating spanwise lift distributions in the form $\frac{cc_l}{2b}$ for $\alpha_\delta\delta=1$ and multiplying the results by $\frac{2b}{cC_{L_{\alpha_e}}}$. A simpler but less accurate way of estimating these values consists in using the modified strip theory, which is also used in this report for the calculation of the lift due to structural deformations, until suitable aerodynamic influence coefficients are available. This approximation implies that the elements of $\left\{\frac{c_l}{C_{L_{\alpha_e}}}\right\}_\delta$ are 0 for stations not covered by the aileron and 1 for stations covered by the aileron. However, in order to take into account the location of the inboard and outboard extremities of the aileron with the relatively few stations used in the analysis, equivalent values of $\alpha_\delta\delta$ have to be used. These values, referred to as equivalent δ values, are given in figure 3. They are intended to give a rounded-off distribution of $\left\{\frac{c_l}{C_{L_{\alpha_e}}}\right\}_\delta$ which has approximately the same area and the same moment about the root as the unmodified strip-theory distribution. The equivalent δ values of figure 3 pertain to actual values of $\alpha_\delta\delta$ equal to 1; they apply to ailerons which extend from $\frac{\eta_i}{b'/2}$ to the tip but can be combined to apply to any aileron configuration. Several examples are listed in the following table for the six-point method, the values of $\alpha_\delta\delta$ being 1 and the equivalent values being read from figure 3(a) as 0.716 for $\frac{\eta_i}{b'/2}=0.55$ and as 0.293 for $\frac{\eta_i}{b'/2}=0.95$:

Aileron ends	Case 1	Case 2	Case 3	Case 4	Case 5
$\frac{\eta_i}{b'/2}$	0.55	0.95	0.55	0	0
$\frac{\eta_o}{b'/2}$	1.00	1.00	.95	1.00	.55
$\frac{\eta}{b'/2}$	$\left\{\frac{c_l}{C_{L_{\alpha_e}}}\right\}_\delta$ according to modified strip theory				
	Case 1	Case 2	Case 3	Case 4	Case 5
0	0	0	0	1	1
.20	0	0	0	1	1
.40	0	0	0	1	1
.60	.716	0	.716	1	.284
.80	1	0	1	1	0
.90	1	.293	.707	1	0

The values of case 3 are obtained from those of cases 1 and 2 and the values for case 5, from the ones of cases 1 and 4.

CALCULATION OF THE MATRICES

A brief introduction to matrix methods is given in the appendix of reference 1; a fuller treatment is given in reference 5. The numerical constants required in the method of this report are given in reference 1 and in the present report for 6-point and 10-point solutions. The elements of the matrices $[I]$ and $[I']$ are given in table I and those of the matrices $[II]$ and $[II']$, in table II. The matrix $[I]''$ is essentially the double transpose of the matrix $[I]$ and its elements are given in table III. If the structural influence-coefficient method is used, the required matrices $[C_3']$ and $[C_4']$ may be obtained from reference 1.

The matrix $[A]$ is calculated as described in reference 1 and, if desired, by means of the computing forms given in reference 1. The steps in the computation may be summarized as follows:

Step	Operation
①	$[I]'\left\lfloor\frac{(GJ)_r}{GJ}\right\rceil$
②	$[I]'\left\lfloor\frac{(EI)_r}{EI}\right\rceil$
③	$\frac{(GJ)_r}{(EI)_r}\tan^2\Lambda\,[②]$
④	$\frac{w_e}{b'/2}\left(Q_{\alpha_T}-Q_{\alpha_M}\tan\Lambda\right)[1_1']$
⑤	[①]+[③]+[④]
⑥	$[I']\left\lfloor\frac{e_1}{e_{1_r}}\left(\frac{c}{c_r}\right)^2\right\rceil_{sub}$
⑦	[⑤][⑥]
⑧	k[②]
⑨	$\frac{w_e}{b'/2}\frac{b'/2}{e_{1_r}c_r\cos^2\Lambda}Q_{\alpha_M}[1_1']$
⑩	[⑧]−[⑨]
⑪	$[II']\left\lfloor\frac{c}{c_r}\right\rceil$
⑫	[⑩][⑪]
⑬	[A]=[⑦]−[⑫]

where the notation [⑦], for instance, refers to the matrix calculated in step 7. For supersonic speeds four additional steps are required:

6a	$[I]\left\lfloor\frac{e_1}{e_{1_r}}\left(\frac{c}{c_r}\right)^2\right\rceil_{spr}$
7a	[⑤] [6a]
12a	$\frac{(e_{1_r})_{sub}}{(e_{1_r})_{spr}}$[⑬]
13a	[A]=[7a]−[12a]

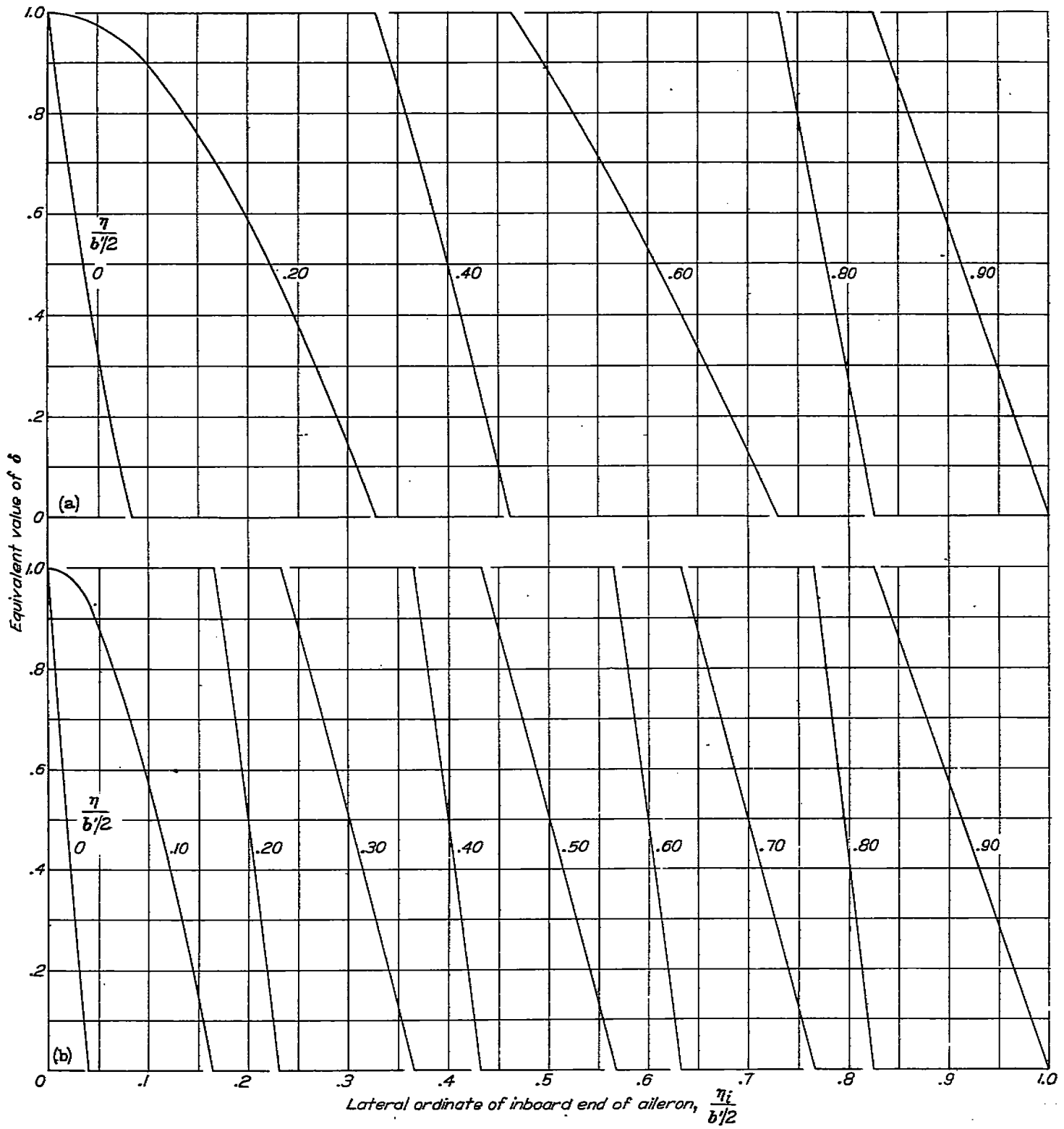

(a) Six-point method.
(b) Ten-point method.

FIGURE 3.—Equivalent values of δ.

To proceed with the calculation of lateral control and of the aileron reversal speed, the auxiliary aeroelastic and the aileron-reversal matrices are then calculated as shown in table IV; the numbering of the steps indicated in the upper left corner of each block is a continuation of the numbering of the steps required to calculate the matrix $[A]$. The auxiliary aeroelastic matrix is obtained in step 15 and the aileron-reversal matrix, in step 20. The value of g required in step 16 is obtained by *post*multiplying the row $[II'_0]\left[\frac{c}{c_r}\right]$ obtained in the step immediately above step 16 by the column $\left\{\frac{c_l}{C_{L_{\alpha_e}}}\right\}_\delta$. On the other hand, the square matrix of step 18 is obtained by *pre*multiplying the row matrix [⑰], which is the same row matrix $[II'_0]\left[\frac{c}{c_r}\right]$ multiplied by $\frac{1}{g}$, by the column $\left\{\frac{c_l}{C_{L_{\alpha_e}}}\right\}_\delta$.

A separate set of calculations from step 14 to step 20, inclusive, has to be performed for subsonic and supersonic speeds; the steps for supersonic speeds can be labeled steps 14a to 20a to follow the pattern set in reference 1. For a 10-point solution, forms similar to those of table IV can easily be drawn up. For the influence-coefficient method a set of computing instructions and computing forms can be based on equations (10) and (11) in the same way as the instructions and forms discussed in this section are based on equations (7), (8), and (18).

Special cases arise when any or all of the values of e_1 or of e_2 are zero. If only e_{1_r} is zero, the value of e_1 at some other point can be used as a reference throughout the analysis and the parameter q^* can be redefined accordingly. The first column of the matrix [⑭] is calculated in this case by multiplying the first column of the matrix [⑤] $[I']$ by the ratio of the value e_{2_r} to the reference value of e_1. Similarly, if some other value of e_1 is zero, say the nth along the span, e_{1_r} is used as a reference but the nth column of [⑭] is calculated by multiplying the nth column of the matrix [⑤] $[I']$ by $\frac{e_{2_n}}{e_{1_r}}\left(\frac{c_n}{c_r}\right)^2$, where e_{2_n} and c_n are the values of e_2 and c at the nth station.

If e_1 is zero along the entire span, some of the computing instructions given in this report, as well as the ones given in reference 1, must be modified somewhat. In table VI (a) of reference 1 the matrix $\left[\frac{e_2}{e_{2_r}}\left(\frac{c}{c_r}\right)^2\right]$ can be entered in the space provided for the $\left[\frac{e_1}{e_{1_r}}\left(\frac{c}{c_r}\right)^2\right]$ matrix. Some of the instructions of table VI(b) of reference 1 and table IV of this report are then modified as follows:

Step 6	$[I']\left[\frac{e_2}{e_{2_r}}\left(\frac{c}{c_r}\right)^2\right]$
Step 9	$\frac{(EI)_r}{(GJ)_r}\frac{w_e}{b'/2}\frac{Q_{\alpha_M}}{\tan\Lambda}[1_1']$
Step 10	[⑨]−[②]
Step 11	As is
Step 12	Omit
Step 13	$[A]_{e_1=0}=$[⑩][⑪]
Step 14	$\frac{e_{2_r}c_r\cos^2\Lambda}{b'/2}\frac{(EI)_r}{(GJ)_r}\frac{1}{\tan\Lambda}$[⑦]
Step 15	$[\bar{A}]=$[⑭]−[⑬]

All other instructions are unaffected.

If e_2 is zero along the span, table IV of this report may be modified as follows:

Step 15	$[\bar{A}]=$[⑫]

Step 14 may be omitted in this case; all other steps in table IV are unaffected.

Similar modifications must also be made if the influence-coefficient method is used.

CALCULATION OF THE AILERON REVERSAL SPEED

The matrix $[A_R]$ is iterated in table V(a) to calculate the critical value of the parameter κq^* and hence the critical speed. The calculation has to be performed once for subsonic speeds and, if the airplane is to fly at transonic and supersonic speeds, once for supersonic speeds. From these critical values, from the definition of the parameters κ and q^*, and from the lift-curve slope the dynamic pressure required for aileron reversal q_R may be calculated and plotted as a function of Mach number. If the actual dynamic pressure for the altitudes of interest is also plotted on the same chart, the lowest intersection of the reversal with a true-dynamic-pressure line will give the reversal Mach number and dynamic pressure at the altitude of the true-dynamic-pressure line.

The matrices $[A_R]$ calculated for the special cases mentioned in the preceding section do not all yield the critical value of the parameter κq^*. When the value of e_1 is zero at the root, the critical value of the parameter κq^* based on the reference value of e_1 will be obtained. If e_1 is zero at some other point along the span or if e_2 is zero along the entire span, critical values of the parameter κq^* will be obtained. In the case where e_1 is zero along the entire span, iteration of the matrix $[A_R]$ calculated by following the instructions of the preceding section will yield the value of the parameter $\kappa\bar{q}$ at reversal.

In some of these special cases, and possibly in other cases as well, the iteration procedure may not converge. In those cases the lowest value of the parameters $(\kappa q^*)_R$ or $(\kappa\bar{q})_R$ is imaginary, so that there is no physical reversal speed corresponding to this value, and the wing under consideration is likely to be safe against reversal (in the speed range under consideration). If the lowest value of the parameter κq^* has the sign opposite to that of the value of e_{1_r} (or the other value of e_1 used as a reference) or if the critical value of $\kappa\bar{q}$ has the sign opposite to that of the sweep angle Λ, the reversal dynamic pressure is negative. In that case the wing also is likely to be safe against reversal, since a negative dynamic pressure cannot be obtained at any real speed.

However, if the wing is to operate at dynamic pressures which correspond to values of κq^* or $\kappa\bar{q}$ much larger than the absolute values of the critical values obtained by iteration, the next higher eigenvalues of the aileron-reversal matrix may have to be calculated by a method such as that given in reference 5, page 143. If the next higher eigenvalue is real and of appropriate sign, it defines the critical aileron reversal speed.

Instead of iterating the matrix $[A_R]$ to calculate $(\kappa q^*)_R$ the determinant of the matrix $[[1]-\kappa q^*[A_R]]$ may be expanded and equated to zero, as noted in reference 1. The result is an equation of the type

$$C_n(\kappa q^*)^n+C_{n-1}(\kappa q^*)^{n-1}+\ .\ .\ .\ +C_1(\kappa q^*)+1=0$$

where n is the order of the matrix—that is, 6 or 10 in the case of a 6-point or 10-point solution, respectively. Solution of this equation yields n values of κq^*; the lowest real value with the appropriate sign is the one that defines the critical reversal speed. Instead of actually expanding the determinant, however, the coefficients C_1, C_2, . . . C_n can be obtained in terms of the traces of the powers of the maxtrix $[A_R]$, the trace of a matrix being the sum of the elements on its principal diagonal, and the nth power of the matrix $[A_R]$ being the matrix obtained by multiplying $[A_R]$ by itself $n-1$ times. If s_m is the trace of $[A_R]^m$, then

$$C_1=-s_1$$

$$C_2=-\frac{1}{2}(C_1s_1+s_2)$$

$$C_3=-\frac{1}{3}(C_2s_1+C_1s_2+s_3)$$

. . . . .

$$C_n=-\frac{1}{n}(C_{n-1}s_1+C_{n-2}s_2+\ .\ .\ .\ +C_1s_{n-1}+s_n)$$

Unless certain types of automatic computing machinery are available, the iteration procedure is generally preferable to the procedure based on the expansion of the determinant.

CALCULATION OF CONTROL POWER AND MANEUVERABILITY

The calculation of the twist distribution for a given aileron deflection may be carried out in table V (b), which is similar to table VI (b) of reference 1. The matrix $[[1]-\kappa q^*[A]]$ is entered at the left, and the column $\left\{\frac{c_l}{C_{L_{\alpha_e}}}\right\}$ is entered at the right. This column is *pre*multiplied by the $[\bar{A}]$ matrix obtained in step 15 or step 15a and is entered in the second column at the right, which in turn is multiplied by $-\kappa q^*$ to yield the third column. The simultaneous equations with the coefficients at the left and the knowns at the right (the third column) are then solved for the unknown α_s values. If preferred, an iterative solution of the type discussed in reference 1 may be used instead of Crout's method (reference 6) for which table V is set up. A computing form similar to that of table VII (c) of reference 1 may be used for this purpose.

If the same values of κq^* are selected as were used in the calculation of the aerodynamic loading by the method of reference 1, the $[[1]-\kappa q^*[A]]$ matrix is already available. If, in addition, Crout's method of solving simultaneous equations has been used to solve the simultaneous equations, part of the auxiliary matrix is also available so that calculation of the α_s values for the aileron loading requires very little time. However, the iterative solution does not have this advantage.

In some of the special cases discussed in the preceding sections, care must be taken to use the proper parameters in conjunction with the matrices calculated for these special cases. In the case where e_{1_r} is zero, the values of κq^* must be based on the reference value of e_1 selected in calculating the matrix; in the case where e_1 is zero along the entire span, the parameter $\kappa\bar{q}$ must be used instead of κq^* in table V (b).

The resulting α_s values may be added algebraically to the values of $\left\{\frac{c_l}{C_{L_{\alpha_e}}}\right\}_\delta$, multiplied by $\frac{c_r}{\bar{c}}$ and $\left[\frac{c}{c_r}\right]$ as indicated in steps 4, 5, and 6 of table V(b), and plotted over the span to yield the net aerodynamic load distribution $\left\{\frac{cc_l}{\bar{c}C_{L_{\alpha_e}}}\right\}_{\delta_{fw}}$ which pertains to a unit value of $\alpha_\delta\delta$ on the flexible wing. The rolling-moment coefficient due to this forcing loading (over both wings) may be obtained from a dimensionless form of equation (13)

$$C_{l_w}=\frac{1}{2}C_{L_{\alpha_e}}\left(\frac{b'}{b}\right)^2\lfloor II'_0\rfloor\left\{\frac{cc_l}{\bar{c}C_{L_{\alpha_e}}}\right\}_{\delta_{fw}} \tag{19}$$

This coefficient, which is a direct measure of the rolling power, is seen to be dependent only on q/q_D (except for the factor $C_{L_{\alpha_e}}$) since $\frac{q}{q_D}=\frac{\kappa q^*}{(\kappa q^*)_D}$ and $(\kappa q^*)_D$ is constant for a given speed range.

The rolling maneuverability depends not only on the rolling power but also on the damping in roll. The rate of roll per unit aileron deflection (measured in a plane parallel to the plane of symmetry) is given by

$$\left(\frac{pb}{2V}\right)_{\delta=1}=\alpha_\delta\frac{C_{l_\delta}}{C_{l_p}} \tag{20}$$

where C_{l_δ} is the forcing coefficient calculated from equation (19) (if the contributions of the pressures on the fuselage are neglected) and C_{l_p} is the damping coefficient calculated from equation (19) with a column of values of $\left\{\frac{cc_l}{\bar{c}C_{L_{\alpha_e}}}\right\}$ calculated by the method of reference 1 for a case where $\alpha_\sigma=\frac{y}{b/2}$. If modified strip theory is used, the desired column is

$$\left\{\frac{cc_l}{\bar{c}C_{L_{\alpha_e}}}\right\}=\frac{c_r}{\bar{c}}\left[\frac{c}{c_r}\right]\{\{\alpha_s\}+\{\alpha_\sigma\}\}$$

where α_s is the structural deformation associated with the given values of α_σ.

ILLUSTRATIVE EXAMPLE

The method described in the preceding sections has been used to analyze the lateral maneuverability of the wing considered in the illustrative example of reference 1. The required additional parameters of this wing are presented in table VI (a), which follows the form of table IV (a). Modified strip theory has been used for calculating $\left\{\frac{c_l}{C_{L_{\alpha_e}}}\right\}_\delta$. The equivalent value of δ at the station $\frac{\eta}{b'/2}=0.4$ is obtained from figure 3 for the given values of $\frac{\eta_i}{b'/2}$ and $\frac{\eta_o}{b'/2}$. The auxiliary aeroelastic matrix for the subsonic case has been calculated by following the form of table IV(b); the resulting matrix is shown in table VI (b).

The aileron-reversal matrix for the subsonic case is calculated by means of the form of table IV (c). Several of the steps, as well as the result, are shown in table VI (c) for the subsonic case. In these calculations the contribution of the matrix $[I'_1]$ to the matrix $[II'_0]$ has been neglected, so that the matrix $[II'_1]$ has been used instead of the matrix $[II'_0]$, a procedure which is not recommended in general. Iteration of the aileron-reversal matrix (by means of the form of table V(a) or otherwise) yields a value of $(\kappa q^*)_R=2.364$. A similar calculation for supersonic speeds yields a value of $(\kappa q^*)_R=0.1280$. From these two values and the definition of the parameters κ and q^* the dynamic pressure required for reversal has been calculated and is plotted against Mach number in figure 4. Also shown in figure 4 for comparison are the dynamic pressures required for divergence as well as the actual dynamic pressures at sea level and at an altitude of 25,000 feet. Where the dynamic pressure required for reversal is less than the actual dynamic pressure, the aileron control is reversed. For the example wing, reversal is likely to occur at a Mach number of approximately 1.3 at sea level.

The aerodynamic loading due to aileron deflection has been calculated by means of the form of table V(b). For the subsonic case and for $\kappa q^*=0.552$ the $[[1]-\kappa q^*[A]]$ matrix is that shown in table X(b) of reference 1. The three columns to be entered at the right of table V(b), as well as the four columns obtained at the bottom of table V(b), are as follows:

①	②	③
$\left\{\frac{c_l}{C_{L_{\alpha_e}}}\right\}_\delta$	$[A]\{①\}$	$-\kappa q^*\{②\}$
0	0	0
0	.1890	−.1043
.265	.5100	−.2815
1	.8217	−.4536
1	1.0273	−.5671
1	1.0656	−.5882

⑥	⑤	④	Final matrix
$\frac{c_r}{\bar{c}}\{⑤\}$	$\left[\frac{c}{c_r}\right]\{④\}$	$\{①\}+\{\alpha_e\}$	$\{\alpha_e\}$
0	0	0	0
−.080	−.063	−.070	−.0699
.067	.053	.065	−.1999
.599	.473	.061	−.3392
.435	.344	.552	−.4477
.379	.300	.523	−.4773
$[II'_1]\{⑥\}=0.179$			

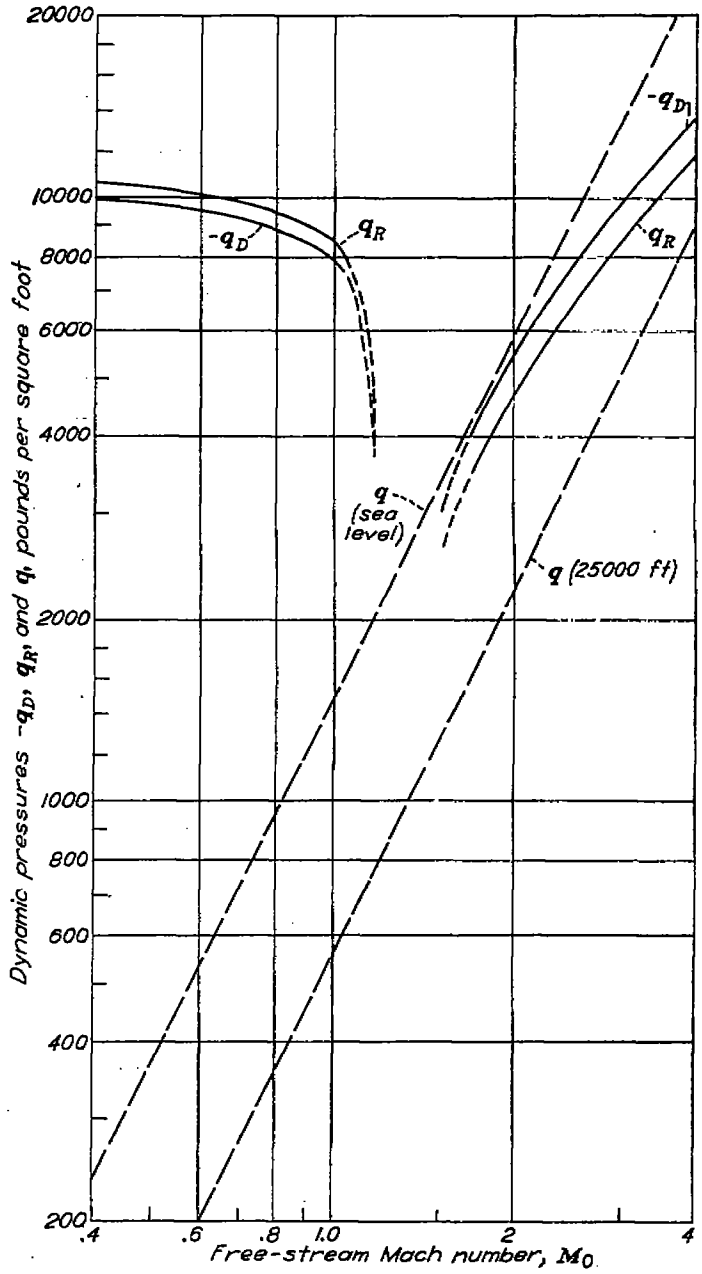

FIGURE 4.—Effect of Mach number on the divergence and aileron-reversal dynamic pressures of the example wing.

The lift distribution due to aileron deflection

$$\left\{\frac{cc_l}{\bar{c}C_{L_{\alpha_e}}}\right\}_\delta=\frac{c_r}{\bar{c}}\left[\frac{c}{c_r}\right]\left\{\frac{c_l}{C_{L_{\alpha_e}}}\right\}_\delta$$

obtained by using the modified strip-theory values of $\left\{\frac{c_l}{C_{L_{\alpha_e}}}\right\}_\delta$ is plotted in figure 5. For the flexible wing the lift distributions due to the calculated twist distributions, such as the one shown in the next to the last column of the foregoing tabulation, must be added algebraically to the lift distribution due to aileron deflection. This addition is best performed by first plotting the lift distributions due to twist

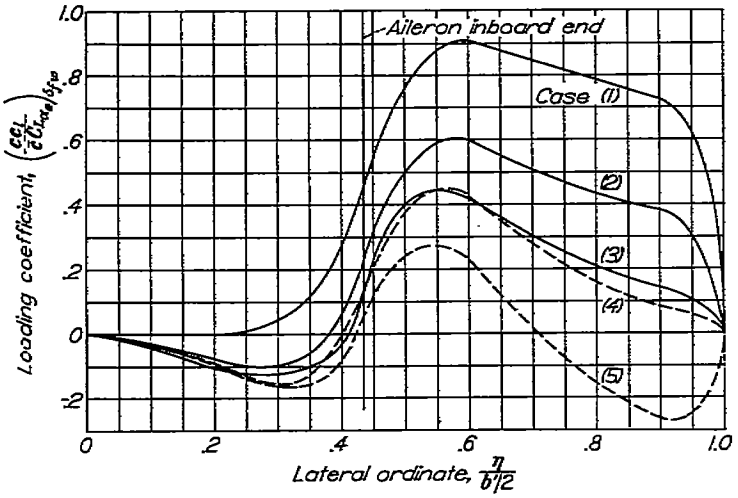

Case	q/q_D	q/q_R	Condition
1	0	0	Subsonic
2	−0.25	0.224	Subsonic
3	−0.50	0.467	Subsonic
4	−0.50	0.577	Supersonic
5	−1.00	1.154	Supersonic

FIGURE 5.—Loading of example wing with aileron deflected.

separately and then adding them point for point to the lift distribution due to aileron deflection. The net distributions obtained in this manner for several cases are shown in figure 5. The distribution for case 5 $\left(\text{supersonic speeds}, \frac{q}{q_D}=-1.00\right)$ indicates that the wing is operating at a speed above its reversal speed; from the given values of q^*_D and q^*_R the dynamic pressure for the case of $\frac{q}{q_D}=-1.00$ can be seen to exceed by 15.4 percent the dynamic pressure required for aileron reversal.

The rolling-moment coefficient is obtained from equation (19) or by adding the moments corresponding to the aileron-distribution curve and the twist curve algebraically. (As stated previously, the contribution of $[I'_1]$ to $[II'_0]$ has been neglected in these calculations.) The ratio of the flexible-wing rolling-moment coefficient obtained in this manner to the corresponding rigid-wing rolling-moment coefficient is plotted in figure 6 (a) against the ratio $-q/q_D$; for the rigid wing the value of C_{l_δ} at subsonic speeds is

$$(C_{l_\delta})_{rw}=0.070C_{L_{\alpha_e}}$$

and at supersonic speeds is

$$(C_{l_\delta})_{rw}=0.026C_{L_{\alpha_e}}$$

The lateral maneuverability is calculated by means of equation (20) with the damping coefficients calculated in reference

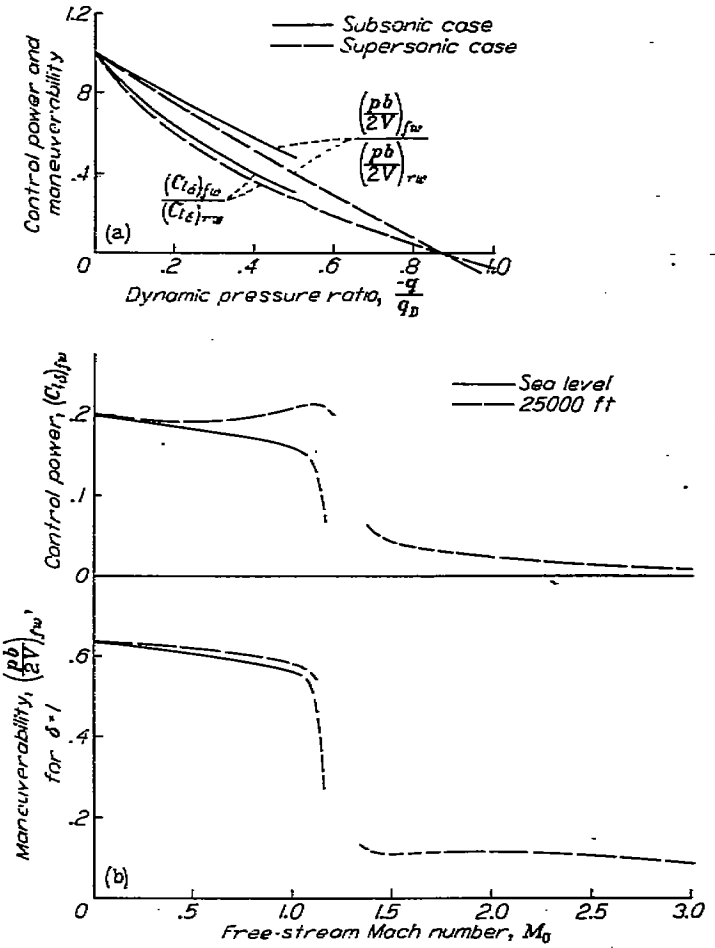

(a) Variation with dynamic pressure ratio.
(b) Variation with Mach number and altitude.

FIGURE 6.—Control power and effectiveness of example wing.

1 and is also plotted in figure 6 (a) as a fraction of the rigid-wing value, which at subsonic speeds is

$$\left(\frac{pb}{2V}\right)_{rw}=0.634$$

and at supersonic speeds is

$$\left(\frac{pb}{2V}\right)_{rw}=0.232$$

Both the maneuverability and the control power become zero at a value of $\frac{q}{q_D}=-0.87$, which is the ratio of the reversal to the divergence dynamic pressure at supersonic speeds, as is shown in figure 4.

Since the ratio q/q_D has been determined as a function of altitude and Mach number in figure 4, the parameters of figure 6 (a) can be plotted as functions of altitude and Mach number, as has been done in figure 6 (b). The maneuverability and, to a lesser extent, the control power are relatively low at supersonic speeds, particularly at low altitudes. Since at high speeds even a small value of $pb/2V$ implies a fairly large

value of the rate of roll p, this situation is not necessarily alarming. The wing in question should have adequate control at all speeds for altitudes greater than about 20,000 feet.

DISCUSSION

The method of this report is based in essence on a numerical integration by means of matrices of the differential equations of structural equilibrium. The actual stiffness distributions, root rotations, and the lift and pitching-moment distributions of the undeformed wing can be taken into account as accurately as they are known. The commonly made simplification of treating the wing as an aggregate of constant-chord segments with all flexibility concentrated at the ends and all forces at the midpoint of the segments is not resorted to in this report. No time-consuming graphical integrations nor trial and error procedures are used. The aileron reversal speed is calculated by means of an iteration, but each cycle of this iteration consists of a single matrix multiplication so that the entire procedure is straightforward in application, and usually the results converge rapidly. If preferred, the iteration procedure can be replaced by an expansion of the determinant of the matrix $[[1]-\kappa q^*[A_R]]$, as outlined in this report.

The purpose of this section is to discuss the assumptions and limitations of the method of this report and to indicate the effect of certain design variables on the aileron reversal speed by means of the results of a few calculations for the example wing and some others related to it.

ASSUMPTIONS AND LIMITATIONS OF THE METHOD

The discussion of the aerodynamic and structural assumptions in reference 1 is also pertinent to the analysis of this report. This discussion may be summarized as follows: All angles of attack, structural deformations, and control deflections must be sufficiently small to give rise only to linear aerodynamic and structural forces. When structural influence coefficients are used, no further assumptions are necessary concerning the structural deformations; when the stiffness curves are used, elementary beam theory as corrected by root rotations must be applicable. If elementary beam theory is inapplicable—that is, if shear deformations, shear lag, and bending-torsion interaction cannot be neglected—a more refined method than elementary beam theory, such as the method of reference 4, can be used to calculate structural influence coefficients which can be used in the method of the present report. When suitable aerodynamic influence coefficients are available, no further assumptions need be made concerning the aerodynamic forces; if no such coefficients are available, the assumption must be made that modified strip theory is sufficiently accurate to calculate the aeroelastic effects of interest.

In the present report additional aerodynamic assumptions must be made, primarily, because although accurate aerodynamic information can be used in the method of this report such information is not available in many instances. For instance, no suitable aerodynamic influence coefficients are available as yet for antisymmetric lift distributions so that modified strip theory has to be used for the lift due to structural deformation. For the lift due to aileron deflection, which is used in the form of the coefficients $\left(\frac{c_l}{C_{L_{\alpha_e}}}\right)_\delta$, the best available information should be used; for unswept wings of moderate or high aspect ratio the method of reference 2 gives accurate results, and for swept wings or wings of low aspect ratio the method of reference 3, with certain modifications explained in reference 6, may be used to calculate the desired coefficients. However, information concerning the parameters α_δ and cp_δ for wings of finite span is very meager; the suggested means of estimating them give results which must be used with some caution. If experimental results are available for these parameters, they can, of course, be used in this method.

Modified strip theory should not in general be used to calculate the coefficients $\left(\frac{c_l}{C_{L_{\alpha_e}}}\right)_\delta$, as was done in the illustrative example. If it is desired to use this approximation, the equivalent δ values of figure 3 may be used to obtain a suitable fairing of the lift-distribution curve at the aileron ends. However, these equivalent values are premised on the use of the $[I']$ and $[II']$ matrices and should not be employed for any other purpose than that indicated herein.

Two additional structural assumptions are also made in this report. In the first place, the angle δ between the wing and the aileron is assumed to be constant along the span. This assumption appears to have been made in almost all of the published investigations into the problem of lateral-control reversal and appears to have yielded satisfactory results; the shorter the aileron and the greater the number of points at which the aileron is supported and at which its hinge moment is taken out, the more nearly true is the assumption. Also, the control linkage is assumed to be stiff so that the aileron angle for a given stick displacement is independent of the dynamic pressure. However, in order to account for the control-linkage deflection, it is necessary only to calculate the ratio of the true aileron angle at a given dynamic pressure to that at zero dynamic pressure for the same stick position. The calculated control moment and maneuverability must then be reduced by this factor to get values of these quantities for a given stick displacement. Since deformations of the control linkage only affect the aileron effectiveness, they have no bearing on the reversal speed. On the other hand, these deformations may lead to aileron divergence for wings with heavily overbalanced ailerons. This problem, as well as the problem of wing-aileron divergence, has not been considered in the present analysis.

The fuselage and tail do not contribute any appreciable amounts to either the control or the damping moment so that their effects may ordinarily be neglected for the purpose of lateral-control calculations. Similarly, the effect of wing camber does not enter into the problem, because the only important effect of camber is to give the flexible wing a symmetrical lift distribution if it is set at the angle of attack which would give zero lift for the rigid wing; this symmetrical lift distribution has no effect on the lateral-control problem.

As in reference 1, the effects of the inertia loading on the aerodynamic loading have not been considered explicitly in the analysis of this report. As pointed out in reference 1, however, the structural deformations due to the inertia loading may be calculated conveniently by means of the integrating matrices and then be considered as part of the geometrical angles of attack. This procedure may be applied in the case of a rolling wing to determine the change in rolling moment for a unit rolling acceleration at any given Mach number and dynamic pressure. This rolling moment must be taken into account in estimating the rolling accelerations due to a given forcing moment at any time before the steady-roll condition is reached.

At transonic speeds there is considerable uncertainty in the aerodynamic parameters. The control power is directly proportional to the value of the parameter $c_{l_\delta}=\frac{dc_l}{d\delta}$, which may be quite low in the transonic region due to the fact that the aileron is located in a region of separated flow. The method of this report is applicable to this case if the value of c_{l_δ} is known for the rigid wing and if the aerodynamic forces due to aileron deflection and due to twist can be superimposed linearly. If, for instance, the decrease in this parameter due to flow separation is 40 percent at a given Mach number and if the loss in control power due to wing flexibility amounts to 20 percent, then the total loss is 52 percent. However, the loss in maneuverability due to the decrease in c_{l_δ} may be much less than the loss in control power, since a decrease in c_{l_δ} is usually accompanied by a decrease in c_{l_α} and $C_{L_{\alpha_e}}$ and hence in the coefficient of damping in roll.

Should the value of the parameter c_{l_δ} decrease to zero or reverse, aileron reversal will occur. This type of reversal is altogether different from the type of reversal discussed in this report since it is due entirely to aerodynamic action, whereas the reversal of concern in this report is due to aeroelastic action. Both types of reversal are largely independent of each other; aerodynamic reversal is likely to occur at a given Mach number regardless of the stiffness of the wing, whereas aeroelastic reversal will occur ordinarily at a different speed which is unaffected by the aerodynamic effectiveness.

EFFECTS OF SOME DESIGN VARIABLES ON THE AILERON REVERSAL SPEED

Some general effects of sweep and of the moment arms e_1 and e_2 on the aeroelastic reversal speed may be of interest. The ratio of the reversal parameter $(\kappa q^*)_R$ of a given wing to that of the unswept wing obtained by rotating the given wing $(\kappa q^*)_{R_0}$ is shown in figure 7 (a) plotted against a function of the sweep angle for subsonic and supersonic speeds; the two curves were obtained by considering the wing of the illustrative example to be rotated in such a manner as to keep the parameters $\frac{e_{1_r}c_r\cos^2\Lambda}{b'/2}$ and $\frac{(EI)_r}{(GJ)_r}$ as well as the chord, stiffness, and moment-arm distributions e_1 and e_2 constant.

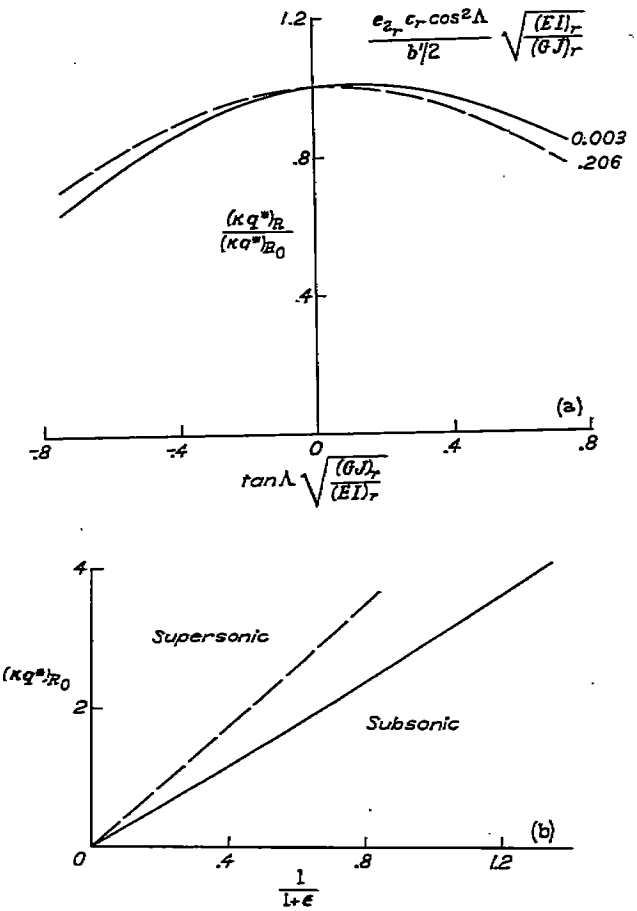

(a) Effect of sweep on reversal parameter $(\kappa q^*)_R$.
(b) Effect of moment-arm ratio ϵ on reversal parameter $(\kappa q^*)_{R_0}$ for unswept wings.
FIGURE 7.—Effects of sweep and moment-arm ratio on reversal speed.

Both sweepback and sweepforward apparently tend to decrease the reversal parameter and hence the reversal speed. At supersonic speeds or, more specifically, at small values of the parameter $\frac{e_{2_r}c_r\cos^2\Lambda}{b'/2}\sqrt{\frac{(EI)_r}{(GJ)_r}}$ the reversal speed for the sweptforward wing is somewhat lower than that of the sweptback wing; whereas at higher values of the parameter the variation of the reversal speed with the sweep parameter $\tan\Lambda\sqrt{\frac{(GJ)_r}{(EI)_r}}$ is more nearly symmetrical with respect to the zero-sweep case. There are some indications that this behavior is not typical of all wings but rather is due to the fairly large variation of the values of e_1, e_2, and ϵ over the span of the example wing. In general it appears that, for small values of the moment-arm parameter $\frac{e_{2_r}c_r\cos^2\Lambda}{b'/2}\sqrt{\frac{(EI)_r}{(GJ)_r}}$, the variation of the reversal speed with the sweep parameter $\tan\Lambda\sqrt{\frac{(GJ)_r}{(EI)_r}}$ should be nearly symmetrical and that, for large values of the moment-arm parameter, the reversal speed should tend to be lower for sweptback wings than for sweptforward wings.

The variation of the reversal speed of an unswept wing with the moment-arm ratio is shown in figure 7 (b) for wings which have the same distributions of the parameters e_1/e_{1_r} and e_2/e_{2_r} along the span but have different values of e_{1_r} and

e_{2_r}. The parameter $(\kappa q^*)_{R_0}$ is plotted against the ratio $\frac{1}{1+\epsilon}$, where the value of ϵ is selected at the midaileron station. It is seen that the plot is linear for both the subsonic and supersonic case. The difference in these cases is due to the different variations of e_1 and e_2 along the span; if the variations were the same or if e_1 and e_2 were constant along the span, the two lines of figure 7 (b) would coincide. Since the reversal parameter $(\kappa q^*)_{R_0}$ is proportional to $\frac{1}{1+\epsilon}$ and since the reversal dynamic pressure is directly proportional to the reversal parameter and inversely proportional to the value e_{1_r} (by definition of the parameter κq^*), it follows that the reversal dynamic pressure is approximately proportional to the ratio $\frac{1}{e_1+e_2}$. From figure 1 it is seen that the sum of e_1 and e_2 represents the distance from the aerodynamic center to the center of pressure of the lift due to aileron deflection and is independent of the location of the elastic axis. This fact corroborates the commonly made observation that the reversal speed is independent of the location of the elastic axis in the case of unswept wings.

The control power and maneuverability cannot be related to the structural and geometric parameters in as relatively simple a manner as the reversal speed. The control power is a function of both the ratio q/q_R and the ratio q_R/q_D; it normally decreases with q/q_R, the rate of decrease being slow at first and then more rapid for positive values of q_R/q_D (which would generally be obtained for unswept and sweptforward wings) and being rapid at first and then slower for negative values of q_R/q_D (which would generally be obtained for sweptback wings). The variation of the maneuverability should generally be similar to that of the control power since the damping coefficient decreases (or in the case of unswept and sweptforward wings increases) steadily with q/q_D and is independent of q_R/q_D.

From the calculations for the example wings it appears that the control power and maneuverability of sweptback wings tend to be relatively low, particularly at supersonic speeds. A combination of high sweep and large moment arm e_2 may lead to an undesirably low maneuverability. Of course, any increase in the purely aerodynamic effectiveness α_δ of the aileron-airfoil combination results in a proportional increase in the lateral-control effectiveness. At supersonic speeds α_δ is proportional to the aileron-chord ratio c_a/c, so that an increased aileron chord results in greater maneuverability; at subsonic speeds an increase in the aileron chord is less effective. Another obvious means of raising the reversal speed and of increasing the control power is to increase either the torsional stiffness or the bending stiffness of the structure. In some cases, however, the increase of the reversal parameter $(\kappa q^*)_R$ due to a change in the parameter $\tan \Lambda \sqrt{\frac{(GJ)_r}{(EI)_r}}$ (see fig. 7 (a)) produced by a decrease in the torsional stiffness $(GJ)_r$ may be so rapid as to cause a net increase in the reversal speed.

If the sweep, the moment arm e_2, the stiffness, and the aileron effectiveness cannot be changed sufficiently to increase the maneuverability, it may be necessary to resort to uncoventional control devices. Leading-edge ailerons, for instance, have negative values of the moment arm e_2, so that wings equipped with them tend to reverse at very high speeds, if at all. This type of configuration has the additional advantage of relatively high effectiveness at transonic speeds. The effectiveness of leading-edge ailerons at subsonic speeds is so low, however, that they would have to be used in conjunction with trailing-edge ailerons to assure satisfactory lateral control at low subsonic speeds; furthermore, they pose some other aerodynamic as well as structural and mechanical problems. Similarly, from an aeroelastic point of view spoilers appear attractive because they tend to have small or negative values of e_2, but they also pose certain design problems. Consequently, both these devices require careful consideration before they are used to alleviate aeroelastic difficulties in any specific case.

CONCLUDING REMARKS

A method has been presented for calculating the effectiveness and the speed of reversal of lateral control as well as of the aerodynamic loading and the rolling moment produced by aileron deflection on swept flexible wings of arbitrary stiffness.

It has been shown that the aileron reversal speed decreases with both sweptback and sweptforward wings and that the effectiveness of conventional aileron configurations on sweptback wings at supersonic speeds tends to be relatively low. The control effectiveness and the resulting maneuverability of the airplane may be increased by varying some of the design parameters such as the structural stiffness and, if necessary, resorting to unconventional control devices, such as leading-edge ailerons or spoilers.

Langley Aeronautical Laboratory,
National Advisory Committee for Aeronautics,
Langley Field, Va., *April 5, 1951.*

REFERENCES

1. Diederich, Franklin W.: Calculation of the Aerodynamic Loading of Swept and Unswept Flexible Wings of Arbitrary Stiffness. NACA Rep. 1000, 1950.
2. Multhopp, H.: Die Berechnung der Auftriebsverteilung von Tragflügeln. Luftfahrtforschung, Bd. 15, Lfg. 4, April 6, 1938, pp. 153–169. (Available as R.T.P. Translation No. 2392, British M.A.P.)
3. Weissinger, J.: The Lift Distribution of Swept-Back Wings. NACA TM 1120, 1947.
4. Kuhn, Paul: Deformation Analysis of Wing Structures. NACA TN 1361, 1947.
5. Frazer, R. A., Duncan, W. J., and Collar, A. R.: Elementary Matrices and Some Applications to Dynamics and Differential Equations. The Macmillan Co., 1946.
6. DeYoung, John: Spanwise Loading for Wings and Control Surfaces of Low Aspect Ratio. NACA TN 2011, 1950.

TABLE I.—VALUES OF THE INTEGRATING MATRICES [I] AND [I']

(a) Six-Point Solution

[I]

$\frac{\eta}{b'/2}$	0	.2	.4	.6	.8	.9	1.0
0	0.06667	0.26667	0.13333	0.26667	0.10000	0.13333	0.03333
.2	−.01667	.13333	.15000	.26667	.10000	.13333	.03333
.4	0	0	.06667	.26667	.10000	.13333	.03333
.6	0	0	−.01667	.13333	.11667	.13333	.03333
.8	0	0	0	0	.03333	.13333	.03333
.9	0	0	0	0	−.00833	.06667	.04167
1.0	0	0	0	0	0	0	0

[I']

$\frac{\eta}{b'/2}$	0	.2	.4	.6	.8	.9
0	0.06667	0.26667	0.13333	0.26667	0.09333	0.15085
.2	−.01667	.13333	.15000	.26667	.09333	.15085
.4	0	0	.06667	.26667	.09333	.15085
.6	0	0	−.01667	.13333	.11000	.15085
.8	0	0	0	0	.02667	.15085
.9	0	0	0	0	−.01886	.09333

(b) Ten-Point Solution

[I']

$\frac{\eta}{b'/2}$	0	.1	.2	.3	.4	.5	.6	.7	.8	.9
0	0.03333	0.13333	0.06667	0.13333	0.06667	0.13333	0.06667	0.13333	0.06000	0.15085
.1	−.00833	.06667	.07500	.13333	.06667	.13333	.06667	.13333	.06000	.15085
.2	0	0	.03333	.13333	.06667	.13333	.06667	.13333	.06000	.15085
.3	0	0	−.00833	.06667	.07500	.13333	.06667	.13333	.06000	.15085
.4	0	0	0	0	.03333	.13333	.06667	.13333	.06000	.15085
.5	0	0	0	0	−.00833	.06667	.07500	.13333	.06000	.15085
.6	0	0	0	0	0	0	.03333	.13333	.06000	.15085
.7	0	0	0	0	0	0	−.00833	.06667	.06833	.15085
.8	0	0	0	0	0	0	0	0	.02667	.15085
.9	0	0	0	0	0	0	0	0	−.01886	.09333

TABLE II.—VALUES OF THE INTEGRATING MATRICES [II] AND [II′]

(a) Six-Point Solution

[II]

$\frac{\eta}{b'/2}$	0	.2	.4	.6	.8	.9	1.0
0	0	0.05333	0.05333	0.16000	0.08000	0.12000	0.03333
.2	−.00167	.01000	.02500	.10667	.06000	.09333	.02667
.4	0	0	0	.05333	.04000	.06667	.02000
.6	0	0	−.00167	.01000	.01833	.04000	.01333
.8	0	0	0	0	0	.01333	.00667
.9	0	0	0	0	−.00042	.00250	.00292
1.0	0	0	0	0	0	0	0

[II′]

$\frac{\eta}{b'/2}$	0	.2	.4	.6	.8	.9
0	0	0.05333	0.05333	0.16000	0.07314	0.13792
.2	−.00167	.01000	.02500	.10667	.05448	.10775
.4	0	0	0	.05333	.03581	.07758
.6	0	0	−.00167	.01000	.01548	.04741
.8	0	0	0	0	−.00152	.01724
.9	0	0	0	0	−.00108	.00419

(b) Ten-Point Solution

[II′]

$\frac{\eta}{b'/2}$	0	.1	.2	.3	.4	.5	.6	.7	.8	.9
0	0	0.013333	0.013333	0.040000	0.026667	0.066667	0.040000	0.093333	0.046476	0.137920
.1	−.000417	.002500	.006251	.026667	.020000	.053333	.033333	.080006	.040476	.122835
.2	0	0	0	.013333	.013333	.040000	.026667	.066667	.034477	.107750
.3	0	0	−.000417	.002500	.006251	.026667	.020000	.053333	.028476	.092665
.4	0	0	0	0	0	.013333	.013333	.040000	.022476	.077580
.5	0	0	0	0	−.000417	.002500	.006251	.026667	.016477	.062495
.6	0	0	0	0	0	0	0	.013333	.010476	.047410
.7	0	0	0	0	0	0	−.000417	.002500	.004060	.032325
.8	0	0	0	0	0	0	0	0	−.001523	.017240
.9	0	0	0	0	0	0	0	0	−.001077	.004190

TABLE III.—VALUES OF THE INTEGRATING MATRIX [I]

(a) Six-Point Solution

$\frac{\eta}{b'/2}$	0	.2	.4	.6	.8	.9
0	0	0	0	0	0	0
.2	.08333	.13333	−.01667	0	0	0
.4	.06667	.26667	.06667	0	0	0
.6	.06667	.26667	.15000	.13333	−.01667	0
.8	.06667	.26667	.13333	.26667	.06667	0
.9	.06667	.26667	.13333	.26667	.10833	.06667

(b) Ten-Point Solution

$\frac{\eta}{b'/2}$	0	.1	.2	.3	.4	.5	.6	.7	.8	.9
0	0	0	0	0	0	0	0	0	0	0
.1	.04167	.06667	−.00833	0	0	0	0	0	0	0
.2	.03333	.13333	.03333	0	0	0	0	0	0	0
.3	.03333	.13333	.07500	.06667	−.00833	0	0	0	0	0
.4	.03333	.13333	.06667	.13333	.03333	0	0	0	0	0
.5	.03333	.13333	.06667	.13333	.07500	.06667	−.00833	0	0	0
.6	.03333	.13333	.06667	.13333	.06667	.13333	.03333	0	0	0
.7	.03333	.13333	.06667	.13333	.06667	.13333	.07500	.06667	−.00833	0
.8	.03333	.13333	.06667	.13333	.06667	.13333	.06667	.13333	.03333	0
.9	.03333	.13333	.06667	.13333	.06667	.13333	.06667	.13333	.07500	.06667

TABLE IV.—FORM FOR COMPUTATION OF AUXILIARY AEROELASTIC AND AILERON-REVERSAL MATRICES

(a) Parameters Pertinent to Lateral-Control Calculations

$\frac{\eta_i}{b'/2}$=_____ $\frac{\eta_o}{b'/2}$=_____

α_δ=_____

$\frac{\eta}{b'/2}$	$\left(\frac{c_l}{C_{L_{\alpha_e}}}\right)_\delta$	cp_δ	e_2	ϵ
0				
.2				
.4				
.6				
.8				
.9				

	$[\epsilon]$					
$\frac{\eta}{b'/2}$	0	.2	.4	.6	.8	.9
0		0	0	0	0	0
.2	0		0	0	0	0
.4	0	0		0	0	0
.6	0	0	0		0	0
.8	0	0	0	0		0
.9	0	0	0	0	0	

(b) Calculation of the Auxiliary Aeroelastic Matrix

⑭	[⑦] [ε]					
$\frac{\eta}{b'/2}$	0	.2	.4	.6	.8	.9
0	0	0	0	0	0	0
.2						
.4						
.6						
.8						
.9						

⑮	$[\bar{A}]=$[⑫]+[⑭]					
$\frac{\eta}{b'/2}$	0	.2	.4	.6	.8	.9
0	0	0	0	0	0	0
.2						
.4						
.6						
.8						
.9						

(c) Calculation of the Aileron-Reversal Matrix

$\frac{w}{b'}$=_____

$[II'_0]=[II'_1]+\frac{w}{b'}[I'_1]$

$[II'_0]\left[\frac{c}{c_r}\right]$

⑯	$g=\left[[II'_0]\left[\frac{c}{c_r}\right]\right]\left\{\frac{c_l}{C_{L_{\alpha_e}}}\right\}_\delta$ g=_____

⑰	$\frac{1}{g}[II'_0]\left[\frac{c}{c_r}\right]$					

⑱	$\left\{\frac{c_l}{C_{L_{\alpha_e}}}\right\}_\delta$ [⑰]					
$\frac{\eta}{b'/2}$	0	.2	.4	.6	.8	.9
0	0	0	0	0	0	0
.2						
.4						
.6						
.8						
.9						

⑲	[⑮] [⑯]					
$\frac{\eta}{b'/2}$	0	.2	.4	.6	.8	.9
0	0	0	0	0	0	0
.2						
.4						
.6						
.8						
.9						

⑳	$[A_R]=$[⑬]+[⑲]					
$\frac{\eta}{b'/2}$	0	.2	.4	.6	.8	.9
0	0	0	0	0	0	0
.2						
.4						
.6						
.8						
.9						

TABLE V.—FORM FOR SOLUTION OF AEROELASTIC EQUATION FOR LATERAL CONTROL

(a) Reversal

$[A_R]$

$\frac{\eta}{b'/2}$	0	.2	.4	.6	.8	.9
0	0	0	0	0	0	0
.2						
.4						
.6						
.8						
.9						

$\{\alpha_s\}$

$\frac{\eta}{b'/2}$	(1)	(2)	(3)	(4)	(5)	(6)
0	0	0	0	0	0	0
.2	.3000					
.4	.5000					
.6	.7000					
.8	.9000					
.9	1.0000	1.0000	1.0000	1.0000	1.0000	1.0000

$[A_R]\{\alpha_s\}$

$\frac{\eta}{b'/2}$	(1)	(2)	(3)	(4)	(5)	(6)
0	0	0	0	0	0	0
.2						
.4						
.6						
.8						
.9						

$(\kappa q^*)_R =$ _____

(b) Control Power

$\frac{q}{q_D} =$ _____ $q =$ _____ $\kappa q^* =$ _____

$[1]-\kappa q^*[A]$

$\frac{\eta}{b'/2}$	0	.2	.4	.6	.8	.9
0	1.0000	0	0	0	0	0
.2						
.4						
.6						
.8						
.9						

①	②	③
$\left\{\frac{c_l}{C_{L_{\alpha_e}}}\right\}_\delta$	$[\bar{A}]\{①\}$	$-\kappa q^*\{②\}$

Auxiliary Matrices

0	1.0000	0	0	0	0	0
.2						
.4						
.6						
.8						
.9						

$[II'_s]$

$[II'_s]\{⑥\} =$ _____

⑥	⑤	④	Final matrix
$\frac{c_r}{c}\{⑥\}$	$\left[\frac{c}{c_r}\right]\{④\}$	$\{①\}+\{\alpha_s\}$	$\{\alpha_s\}$

TABLE VI.—COMPUTATION OF AUXILIARY AEROELASTIC AND AILERON-REVERSAL MATRICES FOR THE EXAMPLE WING AT SUBSONIC SPEEDS

(a) Parameters Pertinent to Lateral-Control Calculations

$$\frac{\eta_i}{b'/2}=\underline{0.434} \qquad \frac{\eta_o}{b'/2}=\underline{1.000}$$

$$\alpha_\delta=\underline{0.547}$$

$\frac{\eta}{b'/2}$	$\left(\frac{c_l}{C_{L_{\alpha_e}}}\right)_\delta$	cp_δ	e_2	ϵ
0	0	0.250	−0.2020	−1.0000
.2	0	.250	−.1990	−1.0000
.4	.265	.458	.0111	.0563
.6	1.000	.458	.0136	.0701
.8	1.000	.458	.0160	.0833
.9	1.000	.458	.0173	.0906

(b) Calculation of the Auxiliary Aeroelastic Matrix

⑮	$[A]=[⑫]+[⑭]$					
$\frac{\eta}{b'/2}$	0	.2	.4	.6	.8	.9
0	0	0	0	0	0	0
.2	.00414	−.00671	.02541	.08337	.03542	.06345
.4	.00774	−.02181	.04563	.21248	.09966	.18577
.6	.00774	−.02181	.04041	.29601	.17065	.34430
.8	.00774	−.02181	.03443	.31802	.20199	.49812
.9	.00774	−.02181	.03443	.31802	.19534	.54309

(c) Calculation of the Aileron Reversal Matrix

	$[II'_1]\left[\frac{c}{c_r}\right]$				
0	0.04826	0.04325	0.11456	0.04549	0.07917
⑯	$g=[II'_1]\left[\frac{c}{c_r}\right]\left\{\frac{c_l}{C_{L_{\alpha_e}}}\right\}_\delta$ $g=\underline{0.2507}$				
⑰	$\frac{1}{g}[II'_1]\left[\frac{c}{c_r}\right]$				
	0	0.1925	0.1725	0.4570	0.1815	0.3158

⑱	$\left\{\frac{c_l}{C_{L_{\alpha_e}}}\right\}_\delta[⑰]$					
$\frac{\eta}{b'/2}$	0	.2	.4	.6	.8	.9
0	0	0	0	0	0	0
.2	0	0	0	0	0	0
.4	0	.0510	.0457	.1211	.0481	.0837
.6	0	.1925	.1725	.4570	.1815	.3158
.8	0	.1925	.1725	.4570	.1815	.3158
.9	0	.1925	.1725	.4570	.1815	.3158

⑳	$[A_R]=[⑬]+[⑲]$					
$\frac{\eta}{b'/2}$	0	.2	.4	.6	.8	.9
0	0	0	0	0	0	0
.2	−.00414	.04310	.02543	.02857	.00433	.00372
.4	−.00774	.12000	.09385	.10715	.01583	.00695
.6	−.00774	.18000	.15503	.26327	.04642	−.00732
.8	−.00774	.21958	.18440	.38811	.10027	.00400
.9	−.00774	.22695	.19101	.40563	.10911	.04635